The role of the tumor suppressor Lkb1 in energy homeostatis

Mans, L.A.

Chapter 2

The tumor suppressor Lkb1 regulates starvation-induced autophagy under systemic metabolic stress

Laurie A. Mans[1,*], Laia Querol Cano[1,2,*], Jason van Pelt[1], Panagiota Giardoglou[1], Willem-Jan Keune[3] and Anna-Pavlina G. Haramis[1*]

1 Institute of Biology, Leiden University, Sylviusweg 72, 2333 BE, Leiden, The Netherlands
2 Present address: Radboud Institute for Molecular Life Sciences – Tumour immunology department, Geert Grooteplein 28, 6525 GA Nijmegen, The Netherlands.
3 Department of Biochemistry, Netherlands Cancer Institute, Plesmanlaan 121, 1066 CX Amsterdam, The Netherlands.
* These authors contributed equally to the manuscript

Scientific Reports. 2017 Aug 4; 7(1): 7327.

Abstract

Autophagy is an evolutionarily conserved process that degrades cellular components to restore energy homeostasis under limited nutrient conditions. How this starvation-induced autophagy is regulated at the whole-body level is not fully understood. Here, we show that the tumor suppressor Lkb1, which activates the key energy sensor AMPK, also regulates starvation-induced autophagy at the organismal level. Lkb1-deficient zebrafish larvae fail to activate autophagy in response to nutrient restriction upon yolk termination, shown by reduced levels of the autophagy-activating proteins Atg5, Lc3-II and Becn1, and aberrant accumulation of the cargo receptor and autophagy substrate p62. We demonstrate that the autophagy defect in *lkb1* larvae can be partially rescued by inhibiting mTOR signalling but not by inhibiting the PI3K pathway. Interestingly, mTOR-independent activation of autophagy restores degradation of the aberrantly accumulated p62 in *lkb1* larvae and prolongs their survival. Our data uncover a novel critical role for Lkb1 in regulating starvation-induced autophagy at the organismal level, providing mechanistic insight into metabolic adaptation during development.

Introduction

Autophagy is a highly conserved, multi-step intracellular process of self-degradation. Under basal conditions, autophagy eliminates damaged proteins and organelles from cells, serving a housekeeping/recycling function. However, upon metabolic stress, starvation-induced autophagy serves to provide substrates for biosynthesis and energy production in order to maintain cellular homeostasis (Kuma et al., 2004; Rabinowitz and White, 2010). The importance of autophagy for cellular and organismal health is showcased by the fact that defects in autophagy have been linked to neurodegeneration, cancer, aging and metabolic syndrome (Rabinowitz and White, 2010).

Starvation-induced autophagy promotes survival in the *Drosophila* fat body (Scott et al., 2004) and in *Caenorhabditis elegans* (Kang et al., 2007). A critical role for autophagy in surviving the metabolic stress at birth has also been demonstrated in mammals: mice deficient in Atg5 (autophagy protein 5, an E3 ubiquitin ligase necessary for autophagosomal elongation) survive fetal development, but die within one day after birth, exhibiting severe hypoglycaemia and hypolipidaemia (Kuma et al., 2004). However, the regulation of systemic starvation-induced autophagy is not well understood.

Autophagy-induction in response to energetic stress is triggered by the activation of AMP activated protein kinase (AMPK) (Fleming et al., 2011; Galluzzi et al., 2014), a key, evolutionarily conserved energy sensor. AMPK activation restores energy homeostasis at the cellular and organismal levels (Hardie et al., 2012a) by many different pathways, including via inhibition of the mechanistic target of rapamycin (mTOR) (Shaw et al., 2004a), a conserved serine-threonine kinase involved in nutrient sensing, growth and proliferation (Laplante and Sabatini, 2012a; Polak and Hall, 2009). AMPK itself is activated by multiple mechanisms including phosphorylation by the tumor suppressor LKB1/STK11 kinase in response to increased AMP or ADP levels in the cell (Hawley et al., 2003; Shaw et al., 2004b). Because of the role of AMPK as a central energy checkpoint in the cell, these findings link LKB1 signalling to energy metabolism control, positioning LKB1 as a critical mediator of the effects of low energy on cell viability (Liang et al., 2007; Shaw et al., 2004b). Accordingly, cells lacking LKB1 undergo apoptosis under metabolic stress as they are unable to respond to energy deficiency and restore homeostasis (Shaw et al., 2004b). LKB1/AMPK signalling is also important for long-term survival under nutrient-limiting conditions during C. *elegans* dauer (diapause) stage (Narbonne and Roy, 2009). However, the early embryonic lethality of both *lkb1* mutant (Ylikorkala et al., 2001) and *ampka1/a2* double mutant mice (Laderoute et

al., 2006) has precluded analysis of the *in vivo* role of LKB1/AMPK in physiological processes occurring at later developmental stages in vertebrates, such as during metabolic stress at birth.

The LKB1/AMPK axis is a negative regulator of mTOR signalling (Shaw et al., 2004a) and mTOR signalling is a known inhibitor of autophagy (Mizushima et al., 2008). However, LKB1 also activates 12 other AMPK-related kinases (Lizcano et al., 2004), and many mTOR-dependent and mTOR-independent autophagy regulators exist (Kroemer et al., 2010).

LKB1/AMPK regulation of mTOR has been linked to the regulation of autophagy in different settings, for example in autophagy stimulated by fluid flow over the primary cilium of epithelial cells (Orhon et al., 2016), and in cancer cells (Maiuri et al., 2009). Furthermore, AMPK directly stimulates autophagy via the ULK1/Atg1 phosphorylation (Egan et al., 2011a; Kim et al., 2011). And LKB1 may also stimulate autophagy by stabilizing p27, thereby linking nutrient sensing to cell-cycle progression (Liang et al., 2007). However, whether and how LKB1 signalling regulates systemic starvation-induced autophagy in vertebrates is currently unknown.

The regulation of systemic metabolism and autophagy are often studied in zebrafish because of its small size and vertebrate physiology (Schlegel and Stainier, 2007; Varga et al., 2015). Importantly, fundamental principles of energy homeostasis are highly conserved between humans and zebrafish (Schlegel and Gut, 2015b) (Seth et al., 2013). Autophagy has critical functions during zebrafish embryonic development (Hu et al., 2011), with autophagy-defective animals displaying abnormal heart development (Lee et al., 2014), which is also seen in mice (Meyer et al., 2013). Zebrafish are also a valuable model for studying tissue regeneration, and autophagy has been shown to be required for the regeneration of amputated caudal fins (Varga et al., 2014). Like mammals, zebrafish also experience metabolic stress at birth, when the maternal nutrient supply (yolk) is depleted. The metabolic stress at birth in mammals is accompanied by induction of gluconeogenesis (Gustafsson, 2009; Pilkis and Granner, 1992a) and of autophagy (Heintz, 2004; Kuma et al., 2004). While induction of gluconeogenesis also serves as a mechanism to restore energy homeostasis in zebrafish (Gut et al., 2013), a role for autophagy during this metabolic transition has not been investigated.

We previously used TILLING (Wienholds et al., 2003) to generate zebrafish larvae that carried a point mutation leading to a stop codon in the kinase domain of *lkb1* (*stk11*^{hu1968}). These larvae survived gastrulation and early embryonic development but died prematurely from starvation at 7 to 8 days post-fertilization (dpf). Our experiments, impossible to conduct in mice due to the early embryonic lethality of *Lkb1* knock-out mice (Ylikorkala et al., 2001), established Lkb1 as a critical regulator of whole-body energy homeostasis (van der Velden et al., 2011). Zebrafish *lkb1* larvae are unable to cope with the energetic stress induced upon yolk depletion and fail to adapt their metabolism to lower nutrient levels. *lkb1* larvae are indistinguishable from wild type (wt) siblings while their maternal nutrient supply is still present, until 5-6 dpf. However, they die within 1-2 days following yolk depletion whereas wt larvae can survive without food until 13-14 dpf (Daouk et al., 2011).

The phenotype of *lkb1* zebrafish is reminiscent of the *atg5* knock-out mice that appear normal until birth but die soon after, due to their inability to cope with the metabolic stress at birth (Kuma et al., 2004). This resemblance prompted us to investigate the autophagy status in the *lkb1* larvae to study the role of Lkb1 in regulation of systemic starvation-induced autophagy.

We show that Lkb1-deficient larvae fail to activate autophagy in response to nutrient restriction. Furthermore, we demonstrate aberrant accumulation of the autophagy adaptor and substrate p62 in *lkb1* larvae, confirming impaired autophagy. Genetic or chemical induction of autophagy in *lkb1* larvae prolongs their survival, while suppression of autophagy shortens it. Survival prolongation only occurs when degradation of p62 is restored. We therefore show that autophagy is essential to survive the feeding-fasting transition in zebrafish, and identify Lkb1 as a critical regulator of whole-body starvation-induced autophagy in vertebrates.

Results

Lkb1 larvae fail to activate autophagy under nutrient limitation

To determine if autophagy initiation and maintenance is affected in the *lkb1* larvae we previously generated (van der Velden et al., 2011), we analysed wt and *lkb1* larvae between 5-7 dpf during the metabolic transition following yolk depletion. *lkb1* larvae are indistinguishable from wt larvae up to day 5-6 dpf (van der Velden et al., 2011) (while there is still yolk). We chose this time window also because the morphological *lkb1* phenotype of flattened intestine and darkened liver is apparent at 7 dpf (van der Velden et al., 2011) and the majority of *lkb1* larvae die at 8 dpf (Supplementary Figure S1). Autophagic activity is commonly monitored by accumulation of the membrane-bound form of MAP1LC3B (microtubule-associated proteins 1A/1B light chain 3B, Atg8 in yeast; Lc3B in zebrafish), Lc3-II, which is a ubiquitin-like protein (Sugawara et al., 2004) that localizes in autophagosomal membranes upon induction of autophagy. To enable visualization of Lc3-II accumulation in autophagosomes, we first blocked the fusion of autophagosomes with lysosomes by treating the larvae with 2.5 μM chloroquine (Shintani and Klionsky, 2004) for 14 hrs before analysis.

We found that Lc3-II protein levels were lower in *lkb1* larvae compared to their wt siblings after yolk depletion at 6 and 7 dpf (Fig. 1A). Note that the Lc3 antibody in zebrafish recognizes predominantly the cleaved Lc3B-II form, which still accurately reflects autophagic activity (Mizushima and Yoshimori, 2007) (Supplementary Figure S2A), and we were only able to detect a faint signal for Lc3B-I in zebrafish lysates (Fig. 1A). To verify this result, we used an alternative marker of autophagy by analyzing the expression of Atg5-containing protein complexes during development. We found that while the expression of the common ~56 KD complex was unaffected, the ~47 KD complex, which is indicative of autophagy induction (Varga et al., 2014) was undetectable in the *lkb1* larvae (Figure 1A). Finally, we also assessed the levels of Beclin 1 (Becn1), a protein involved in autophagosome nucleation (Meyer et al., 2013; Mizushima and Klionsky, 2007) and also commonly used as an autophagy indicator. Becn1 expression was also strongly reduced in the *lkb1* larvae (Supplementary Figure S2B). While Lc3-II and Becn1 levels progressively increased in wt larvae between 5-7 dpf, indicating upregulation of autophagy upon yolk termination, *lkb1* larvae did not show such an increase, suggesting they fail to activate autophagy under nutrient limiting conditions (Figure 1A, and Supplementary Figure S2B).

To examine the spatial distribution of autophagy, we performed immunofluorescence analysis with antibodies against Lc3B on transverse liver and intestine sections of *lkb1* and wt larvae at 7 dpf. Lc3B expression was strongly reduced in *lkb1* intestines and livers as compared to their wt counterparts (Figure 1B-E and Supplementary Figure S2E, F), confirming and supporting the immunoblotting results. Furthermore, immunohistochemistry (IHC) against Becn1 on transverse sections of wt and *lkb1* larvae showed markedly reduced Becn1 staining in the *lkb1* larvae compared to their wt counterparts (Supplementary Figure S2C, D).

To further confirm that activation of autophagy is impaired in *lkb1* larvae, we monitored expression levels of the p62 protein (also known as sequestosome 1, (SQSTM1). p62 is an adaptor protein that targets ubiquitinated proteins or organelles that bind to it for selective autophagy (Lamark et al., 2009). Accumulation of p62 has been observed in mouse AMPK-deficient fibroblasts (Egan et al., 2011b), and is associated with liver toxicity in autophagy-deficient mouse liver (Komatsu et al., 2010). p62 itself is also an autophagy substrate, thus accumulation of p62 levels is a marker for impaired autophagy (Rusten and Stenmark, 2010). In agreement with our model that *lkb1* larvae have impaired autophagy, Western blot analysis of p62 levels at 5, 6 and 7 dpf showed progressive accumulation of p62 specifically in the *lkb1* larvae (Figure 1A). IHC performed on transverse sections of lkb1 intestine and liver confirmed a marked accumulation of p62 in *lkb1* larvae, whereas wt siblings were devoid of staining (Figure 1F, G).

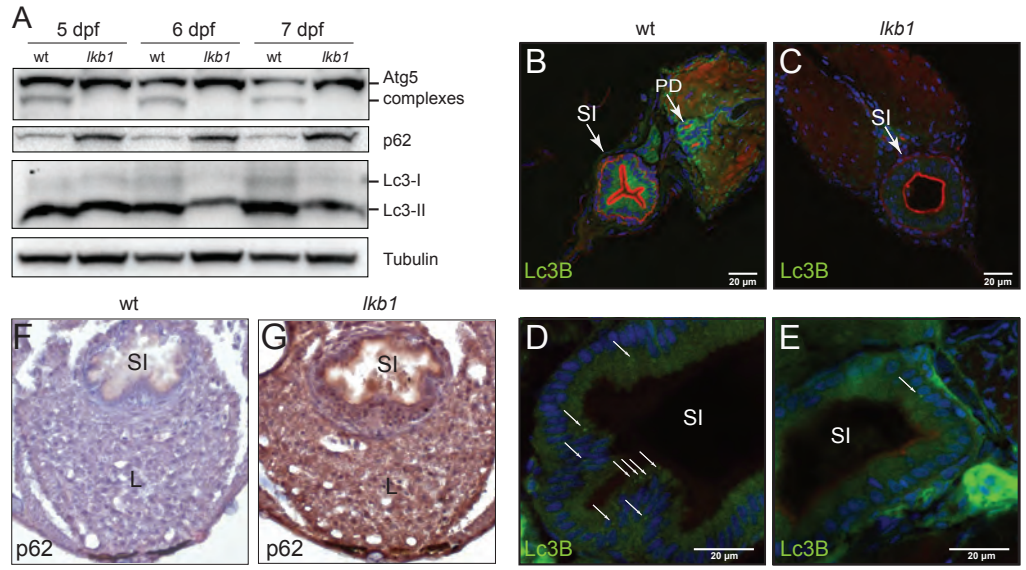

Figure 1. *lkb1* larvae show impaired activation of autophagy following yolk depletion. (A) Representative Western blot analysis of Lc3-II, Atg5, p62 and Tubulin (loading control) in total protein lysates of wt and *lkb1* trunks between 5-7 dpf. Larvae were treated with chloroquine (2.5 µM) for 14 h prior to processing. The marked decrease in Lc3-II and Atg5-containing complexes together with the p62 accumulation indicate impaired autophagy in *lkb1* larvae. *(B-E)* Transverse vibratome sections (150 µm) of intestine of 7 dpf wt and *lkb1* larvae stained with anti-LC3B antibody (green), rhodamine-phalloidin to detect F-actin (red) and DAPI to detect nuclei (blue). Lc3B staining in the *lkb1* intestine is barely detectable *(C, E)* and areas of intense staining were more present in wt sections compared to sections from *lkb1* larvae. *(F, G)* Immunohistochemical analysis of transverse paraffin sections (5 µm) of liver and intestine of 7 dpf wt and *lkb1* larvae reveals high levels of p62 accumulation in *lkb1* liver and intestine. Magnification: 40X. PD: pronephric ducts; L: liver; SI: intestine.

Collectively, these findings demonstrate that whole-body autophagy is impaired in *lkb1* larvae during the feeding-fasting transition in zebrafish, which could contribute to their premature death.

Abrogation of autophagy further decreases survival of *lkb1* larvae

To investigate the effect of inhibiting autophagy on *lkb1* larvae survival prior to yolk depletion, we blocked autophagosome formation using an antisense morpholino oligonucleotide (MO), that targets the translational start-site of *atg5* mRNA (Boglev et al., 2013; Hu et al., 2011), *atg5*MO. We confirmed that injection of *atg5*MO abolishes Atg5 protein expression (Supplementary Figure S3). Atg5-knockdown led to a reduction in Lc3-II levels compared to the negative control in both wt and *lkb1* larvae at 4 dpf, before yolk depletion, confirming autophagy suppression upon *atg5*MO injection (Figure 2A). While all un-injected wt and *lkb1* larvae were alive at 4 dpf, a significant number of *atg5*MO-injected embryos were found dead at that time point. Genotyping all embryos at 4 dpf revealed that 75% of *atg5*MO-injected *lkb1* larvae had died compared to only 25% of *atg5*MO-injected wt larvae (Figure 2B). Thus, *lkb1* larvae, which fail to induce autophagy at the metabolic transition, are also more sensitive to autophagy inhibition at earlier embryonic stages.

The autophagy defect in *lkb1* larvae can be ameliorated by mTOR-dependent and -independent mechanisms

We next investigated the mechanism behind the impaired autophagy observed in the *lkb1* larvae. Signalling through mTOR is known to inhibit autophagy, and we and others have previously reported that mTOR activity is high in wt larvae between 2 and 5 dpf and is downregulated at later stages of larval development (van der Velden et al., 2011) (Boglev et al., 2013; Marshall et al., 2010). This suggests that at the time of yolk depletion, mTOR activity is switched off, enabling the activation of autophagy. It has also been shown in mice that suppression of mTOR activity at birth enables activation of autophagy (Efeyan et al., 2013). We hypothesized that mTOR inactivation was defective in the absence of Lkb1. Therefore, we first assessed the status of mTOR signalling in *lkb1* larvae at the metabolic transition (6 dpf) by analyzing phosphorylation of the mTOR-substrate ribosomal protein S6 (RS6) by Western blot. Total RS6 levels were almost undetectable in wt larvae at this stage, consistent with our previous report (van der Velden et al., 2011). However, both total and phospho- RS6 levels were high in *lkb1* larvae (Figure 3A), indicating active mTOR signalling, which was inhibited by rapamycin treatment. In comparison, in rapamycin-treated 6 dpf wt larvae, we observed increased phospho-RS6 expression (Figure 3A). This could be explained by a known developmental delay caused by chronic mTOR inhibition during development (Makky et al., 2007). Consistent with this, rapamycin-treated wt larvae retained significant amounts of yolk at 7 dpf, demonstrating a delay in larval development (Supplementary Figure S4C).

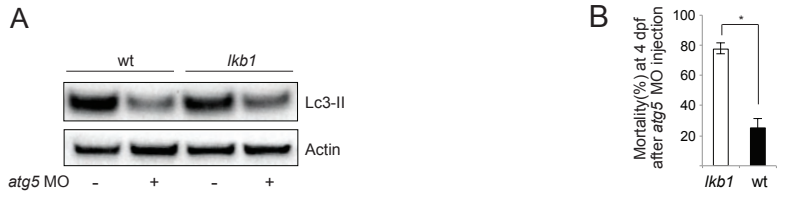

Figure 2. Inhibition of autophagy shortens survival of *lkb1* larvae. (A) Representative Western blot analysis of Lc3-II and Actin (loading control) in total protein lysates of trunks of surviving wt and *lkb1* larvae at 4 dpf that were injected with an atg5MO at the one-cell stage and controls. Larvae were previously treated with 2.5 µM chloroquine for 14 h. Atg5 knock-down led to downregulation of Lc3-II levels in both wt and *lkb1* larvae. *(B)* Graph depicting mortality percentages of atg5MO-injected wt and *lkb1* at 4 dpf. Data represent the means ± standard errors of the means (SEM) and are pooled from two independent experiments (n=80/experiment). * P value < 0,05.

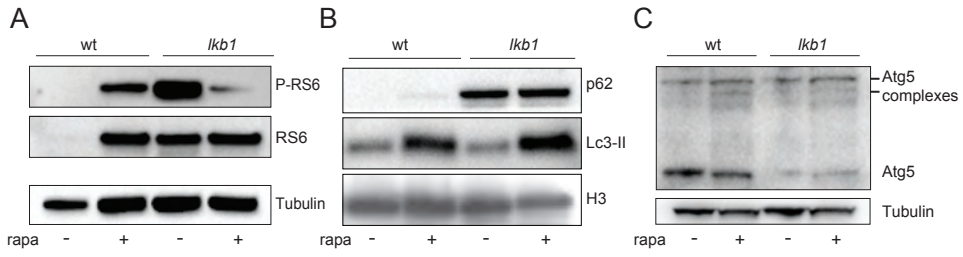

Figure 3. Rapamycin treatment leads to increased Lc3-II accumulation but does not increase Atg5 (complexes) nor restore p62 degradation in *lkb1* larvae. (A) Representative Western blot analysis of Ribosomal protein S6 (RS6), Phospho-RS6 and Tubulin (loading control) in total protein lysates of wt and *lkb1* trunks at 6 dpf that were treated with either 10µM rapamycin from 24 hpf onwards, or with DMSO (negative control). Increased levels of RS6 and P-RS6 are observed in rapamycin-treated wt samples. Total RS6 levels did not change in *lkb1* samples but P-RS6 decreased upon rapamycin treatment. **(B)** Representative Western blot analysis of p62, Lc3-II, and histone H3 (loading control). Larvae were treated with chloroquine (2.5 µM) for 14 h prior to processing. Rapamycin treatment leads to increased Lc3-II levels in both wt and *lkb1* larvae, while p62 accumulation remained high in rapamycin-treated *lkb1* larvae. **(C)** Representative Western blot analysis of Atg5 and Tubulin (loading control). Rapamycin treatment leads to an increase in the amount of the ~47 KD Atg5-containing complex in wt larvae and to a lesser extent in *lkb1* larvae.

To determine whether mTOR signalling mediates the inhibition of autophagy seen in the *lkb1* larvae at 6 dpf, we examined whether rapamycin treatment could restore autophagy in these larvae. We treated wt and *lkb1* embryos with rapamycin from 24 hpf onwards. We have previously reported that rapamycin-treated *lkb1* larvae survive until 9 dpf, but still have a considerable amount of yolk, demonstrating a developmental delay (van der Velden et al., 2011). Rapamycin-treatment resulted in elevated Lc3-II levels in both wt and *lkb1* larvae, at 6 dpf (Figure 3B), indicating that autophagy in the *lkb1* larvae is inhibited, at least in part, by mTOR signalling. The same was also observed when blocking autophagosome-lysosome fusion by chloroquine, which prevents degradation of autophagosome-associated Lc3, allowing monitoring of the autophagic flux (Chittaranjan et al., 2015) (Supplementary Figure S4A, B). However, rapamycin-treatment led to only slight upregulation of Atg5 and complexed Atg5 in *lkb1* larvae (Figure 3C), and was not sufficient to decrease the marked p62 accumulation (Figure 3B). These results suggest that while mTOR inhibition can at least partially restore autophagy in *lkb1* larvae, it cannot entirely alleviate the observed phenotype.

We next analysed the pro-survival PI3K pathway, which in response to external stimuli (growth factors, insulin) also suppresses autophagy, acting upstream of mTOR signalling (Dibble and Cantley, 2015). To this end, we used the small molecule AR-12, an inhibitor of phosphoinositide-dependent kinase (PDK)-1, a component of the PI3K pathway (Chiu et al., 2009), which has been shown to activate autophagy in zebrafish (van der Vaart et al., 2014). Treatment of wt and *lkb1* siblings with AR-12 from 24 hpf onwards, led to accumulation of Lc3-II protein levels in wt but not in *lkb1* larvae at 6 dpf (Figure 4A). Interestingly, AR-12 treatment resulted in upregulation of Atg5 expression and formation of Atg5/12 complexes in wt larvae indicating autophagy induction, but no changes in Atg5 expression were observed in lkb1 larvae (Figure 4B). Furthermore, while p62 protein expression was diminished in wt larvae upon AR-12-mediated activation of autophagy, accumulation of p62 remained unchanged in AR-12-treated *lkb1* larvae (Figure 4A). This indicates that inhibition of the PI3K pathway fails to induce autophagy in mutant larvae.

We next assessed phosphorylation of the mTOR-substrate RS6 upon AR-12 treatment in wt and *lkb1* larvae at 6 dpf. RS6 and phosphorylated RS6 (P-RS6) were not detectable in wt larvae at 6 dpf (Figure 4C), consistent with downregulation of mTOR activity at later developmental stages (here and (van der Velden et al., 2011) (Boglev et al., 2013; Marshall et al., 2010)). AR-12 treatment did not affect the high protein levels of RS6 or P-RS6 seen in the *lkb1* larvae, indicating that they are unsusceptible to PI3K pathway inhibition. In line with the lack of autophagy induction, AR-12 treatment did not enhance *lkb1* survival, as no statistically significant

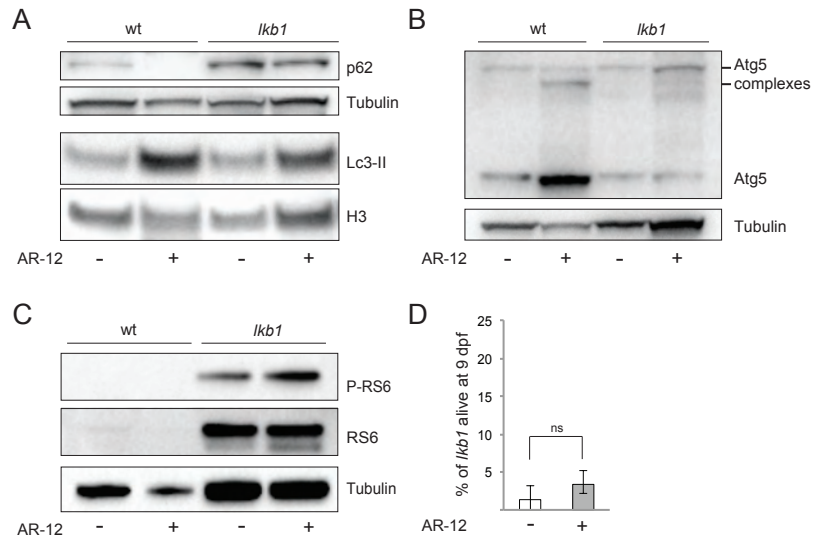

Figure 4. The PI3K-inhibitor AR-12 does not rescue the autophagy defect in *lkb1* larvae and does not prolong their survival. (A) Representative Western blot analysis of Lc3-II, p62 and Histone H3 and tubulin (loading controls) in total protein lysates of wt and *lkb1* trunks at 6 dpf. Larvae were treated with 1 μM AR-12 or DMSO (negative control) from 1 dpf, and with 2.5 μM chloroquine for 14 h prior to processing. AR-12 treatment leads to upregulation of Lc3-II levels in wt larvae but not in *lkb1* larvae. p62 levels remain high in AR-12-treated *lkb1* larvae. **(B)** AR-12 treatment leads to strong increase in the amounts of Atg5 and complexed Atg5 in wt larvae but not in *lkb1* larvae. **(C)** Representative Western blot analysis of Ribosomal protein S6 (RS6), Phospho-RS6 and Tubulin (loading control). Protein levels of total RS6 and of P-RS6 were not affected by AR-12 treatment in *lkb1* larvae. **(D)** Graph depicting survival percentage of *lkb1* larvae alive at 9 dpf. Embryos were treated with 1 μM AR-12 or DMSO from 1 dpf, collected at 9 dpf, and genotyped for the *lkb1* gene. Data represent the means ± standard errors of the means (SEM) and are pooled from three independent experiments P value > 0.05, ns: not statistically significant

differences were observed in the percentage of AR-12 treated *lkb1* larvae alive at 9 dpf compared to DMSO-treated controls (Figure 4D).

Activation of autophagy by an mTOR-independent pathway can be achieved using calpeptin, which inhibits the autophagy inhibitors calpain proteases (Williams et al., 2008). Calpeptin treatment of *lkb1* and wt embryos from 24 hpf onwards, in the presence or absence of chloroquine, enhanced Lc3-II levels in both wt and *lkb1* larvae at 6 dpf (Figure 5A and Supplementary Figure S5) without any effects

on development or yolk absorption. Calpeptin treatment also resulted in upregulation of the amounts of Atg5 and complexed-Atg5 in both wt and *lkb1* larvae (Figure 5B). In contrast to rapamycin treatment, treatment with calpeptin restored p62 degradation in *lkb1* larvae (Figure 5A). Calpeptin treatment had no effect on RS6 phosphorylation in *lkb1* larvae (Figure 5C), consistent with calpeptin being an mTOR-independent autophagy activator (Williams et al., 2008). Moreover, calpeptin-mediated activation of autophagy prolonged survival in 70% of the treated *lkb1* larvae. Specifically, 17.5% of calpeptin-treated *lkb1* larvae survived until 9 dpf, whereas only 1% of vehicle-treated *lkb1* larvae were alive at this point (Figure 5D). Therefore, we conclude that induction of mTOR-independent autophagy results in a more complete restoration of the *lkb1* phenotype compared to that obtained upon inhibition of mTOR signalling.

Accumulation of p62 is an important regulator of autophagy in *lkb1* larvae

Aberrant p62 accumulation appeared as a hallmark of impaired autophagy in *lkb1* larvae, and strongly correlated with survival. While p62 is primarily thought of as a receptor delivering cargo proteins to autophagosomes for degradation, it has also been implicated in enhancing mTOR activity (Duran et al., 2011), thereby regulating autophagy as well. Loss of p62 function led to increased autophagy in mammalian cells and in *C. elegans* (Duran et al., 2011). We thus set out to determine whether reducing p62 levels in larvae would affect autophagy and survival. To this end, we injected a *sqstm1/p62* MO, targeting splicing of *sqstm1/p62* mRNA (van der Vaart et al., 2014), into 1-2-cell stage embryos. RT-PCR confirmed that the *sqstm1/p62* MO blocked *sqstm1/p62* mRNA splicing until at least 5 dpf (Supplementary Figure S6). Western blot analysis of 6 dpf larvae showed decreased p62 expression compared to un-injected controls in both wt and *lkb1* lysates (Figure 6A). This was coupled with increased Lc3-II protein levels, suggestive of autophagy induction.
Knockdown of p62 significantly prolonged *lkb1* survival up to 9 dpf: Approximately 70% of *sqstm1/p62* MO-injected *lkb1* larvae survived to 9 dpf, whereas less than 5% of un-injected *lkb1* larvae were alive at this time-point (Figure 6B). Thus, depleting p62 is sufficient to activate impaired autophagy in *lkb1* larvae and extend survival.

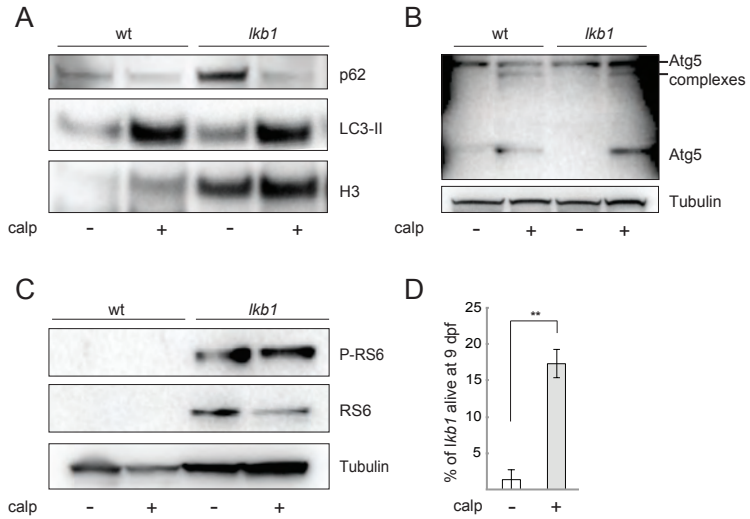

Figure 5. Calpeptin treatment induces autophagy and prolongs survival of *lkb1* larvae. **(A)** Representative Western blot analysis of Lc3-II, p62 and Histone H3 (loading control) in total protein lysates of wt and *lkb1* trunks at 6 dpf. The embryos were treated with 50 µM calpeptin or DMSO (negative control) from 1 dpf onwards, and with 2.5 µM chloroquine for 14 h prior to lysing. Calpeptin treatment leads to upregulation of Lc3-II levels in both wt and *lkb1* larvae. Induction of autophagy by calpeptin also leads to robust downregulation of p62 accumulation in *lkb1* larvae. **(B)** Representative Western blot analysis of Atg5 and Tubulin (loading control). Calpeptin treatment leads stark increase in the amounts of Atg5 and of complexed Atg5 in both wt and *lkb1* larvae. **(C)** Representative Western blot analysis of Ribosomal protein S6 (RS6), Phospho-RS6 and Tubulin (loading control). Calpeptin treatment does not affect RS6 or P-RS6 levels in wt or *lkb1* larvae. **(D)** Graph depicting survival percentage of *lkb1* larvae alive at 9 dpf. Embryos were treated with 50 µM calpeptin or DMSO from 1 dpf, collected at 9 dpf, and genotyped for the lkb1 gene. 17,5% out of a total 25% (70% of calpeptin-treated lkb1 larvae) are alive at 9 dpf. Only 1% of DMSO-treated *lkb1* larvae are alive at 9 dpf. Data represent the means ± standard errors of the means (SEM) and are pooled from three independent experiments (n=100/experiment). ** P value < 0,05.

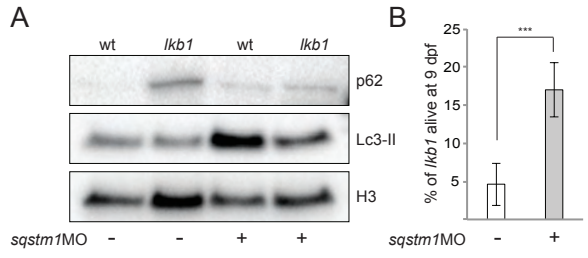

Figure 6. p62 knock-down extends *lkb1* larvae survival. (A) Representative Western blot analysis of p62, LC3-II, and histone H3 (loading control) in total protein lysates of wt and *lkb1* trunks at 6 dpf that were either injected with an sqstm1MO at the one-cell stage or controls. The larvae were treated with 2.5 µM chloroquine for 14 h prior to processing. p62 knock-down leads to increased Lc3-II levels in both wt and *lkb1* larvae. p62 expression in *lkb1* larvae is reduced upon p62 knock-down. **(B)** Graph depicting survival percentage of *lkb1* larvae alive at 9 dpf. Embryos were injected with 0,5 mM sqstm1MO at the one cell stage, collected at 9 dpf, and genotyped for the *lkb1* gene. Data represent the means ± standard errors of the means (SEM) and are pooled from three independent experiments. ***P value ≤ 0.0001.

Discussion

Organisms adapt their metabolism in response to nutrient limitation to restore energy homeostasis and ensure survival. Here, we identify a novel link between metabolic adaptation during development and induction and maintenance of autophagy, mediated by the tumor suppressor Lkb1. Specifically, we use metabolically compromised Lkb1-deficient zebrafish larvae to show that Lkb1 is crucial in the induction of autophagy in response to the metabolic challenge accompanying depletion of the maternal nutrient supply. Our data therefore reveal an essential function for Lkb1 in controlling starvation-induced autophagy at the organismal level in vertebrates.

Overall autophagy levels in *lkb1* larvae are lower compared to those of wt siblings: while expression of autophagy-related proteins is progressively upregulated following yolk depletion in wt larvae, induction of autophagy in *lkb1* larvae is strongly attenuated. Importantly, we demonstrate that genetic and chemical manipulation of autophagy levels significantly impacts *lkb1* larvae survival: inducing autophagy by mTOR-dependent and -independent mechanisms prolongs survival, and suppressing autophagy by Atg5 depletion leads to premature death selectively of the larvae. The increased susceptibility of *lkb1* larvae to Atg5 depletion during development occurred even while the yolk is not yet consumed, suggesting that even though the larvae do not show a morphological phenotype at this embryonic stage, the loss of Lkb1 appears to sensitize them to additional stress. This stress may be specifically autophagy inhibition, or related to alternative mechanisms, as autophagy-independent functions have been reported for several of the autophagy-related genes (Boya et al., 2013; Subramani and Malhotra, 2013), including Atg5 (Yousefi et al., 2006).

Various mechanisms, including mTOR and PI3K signalling, as well as calpains, are known to regulate autophagy (Kroemer et al., 2010), and likely interact at multiple levels. Indeed, our results, together with published work, indicate that all these influence the energy-sensing defect we observe in *lkb1* larvae. We show that activating autophagy by calpeptin, which inhibits the action of the general autophagy inhibitors calpains (Williams et al., 2008), led to robust upregulation of Atg5 expression and restored degradation of p62 in *lkb1* larvae. Thus, calpeptin fully rescued the autophagy defect of the *lkb1* larvae and prolonged their survival. In contrast, while the mTOR-inhibitor rapamycin increased Lc3-II accumulation in *lkb1* larvae, autophagy was not completely restored since p62 still accumulated. This may be due to the high mTOR activity in the larvae that could not be fully blocked by rapamycin treatment under these experimental conditions. In addition, although rapamycin treatment also prolonged *lkb1* survival, we believe this was likely due to a generalized growth delay, evidenced by the presence of a considerable amount of yolk at 7 dpf (this study and (Makky et al., 2007) (van der Velden et al., 2011)), rather than due to partial restoration of autophagy. A developmental delay caused by rapamycin is further supported by the persistence of RS6 expression in rapamycin-treated wt larvae at 7 dpf when mTOR would normally be suppressed (mTOR signalling is suppressed in wt larvae upon yolk depletion at 5-6 dpf (van der Velden et al., 2011) (Boglev et al., 2013; Marshall et al., 2010)).

The autophagy receptor and substrate p62 aberrantly accumulates in *lkb1* larvae indicating deficient autophagy. p62 is also a regulator of autophagy, as it participates in a feed-forward loop in which p62 enhances mTOR activity resulting in reduced autophagy, in turn leading to higher p62 levels in mice (Moscat and Diaz-Meco, 2011). Here we also show that depletion of p62 in *lkb1* larvae leads to activation of autophagy and prolonged survival. This implies that as the amount of p62 decreases due to autophagosomal clearance, its effect on mTOR activity is also reduced, and thus autophagy can be maintained. Furthermore, the aberrant accumulation of p62 in *lkb1* larvae may in itself contribute to their premature lethality, as it has been shown that increased levels of p62 in autophagy-deficient mouse livers cause hepatotoxicity (reviewed in (Moscat and Diaz-Meco, 2011)). Further supporting our hypothesis, in apoptosis-impaired tumor cells with deficient autophagy, p62 accumulation triggers a positive feedback loop for the generation of reactive oxygen species (ROS) leading to enhanced genomic instability and tumorigenesis (Moscat and Diaz-Meco, 2009).

PI3K signalling is a nutrient-sensing pathway that is also implicated in starvation-induced autophagy. Inhibition of the PI3K pathway activated autophagy in wt larvae, but not in *lkb1* larvae, and did not prolong their survival. This is consistent with our previous findings that PI3K signalling is compromised in *lkb1* larvae (van der Velden et al., 2011). We postulate that defective PI3K signalling may contribute to the autophagy defect seen in these larvae. While AMPK is considered a major regulator of metabolism and has an important role in induction of autophagy under energetic stress (Egan et al., 2011b; Kim et al., 2011), it is not overtly activated in wt larvae at 7 dpf (van der Velden et al., 2011); in agreement with these data, studies in mice have also reported that 24 hours of fasting did not lead to significant AMPK activation (Gonzalez et al., 2004; Viollet et al., 2009). Thus, the autophagy defect we describe in *lkb1* larvae is unlikely to be solely attributable to impaired AMPK signalling, and deregulation of additional pathways, such as PI3K signalling and AMPK/mTOR-independent pathways may also be involved. Hence, nutrient-sensing pathways (like the PI3K pathway) and energy-sensing pathways (like

the AMPK pathway) are likely in close cross-talk with each other, not only through their convergence on mTOR signalling but also through different, mTOR-independent mechanisms.

Together, our data indicate that Lkb1 plays an important role in the regulation of autophagy at the whole-organism level, and confirm that autophagy is critical for survival during the metabolic transition in development. Since defects in autophagy are implicated in a plethora of diseases, a better understanding of the upstream regulatory pathways could provide new insights into their pathophysiology.

Materials and Methods

Zebrafish strains and Screening Methods

Zebrafish were handled in compliance with the local animal welfare regulations and were maintained according to standard protocols (zfin.org). Their culture was approved by the local animal welfare committee (DEC) of the University of Leiden and all protocols adhered to the international guidelines specified by the EU Animal Protection Directive 2010/63/EU. Genotype analysis for *lkb1*-mutant embryos was performed as previously described (van der Velden et al., 2011).

Longitudinal analysis of survival of *lkb1* larvae

Larvae obtained from single matings of heterozygous *lkb1* adults were analysed over time. 48-95 larvae were genotyped on 6, 7, 8, 9, 10 and 11 dpf to assess the numbers of *lkb1* larvae alive.

Western Blot analysis

Approximately 20 larvae/sample were lysed (3 µl per larva) in cold lysis buffer (50 mM Hepes, pH 7.6, 50 mM KCl, 50 mM NaF, 5 mM NaPPi, 1 mM EGTA, 1 mM EDTA, 1 mM beta-Glycerophosphate, 1 mM DTT, 1 mM Vanadate, 1 % NP40) containing phosphatase and proteinase inhibitors. Lysates were pestled for 5 min, sonicated for 30 seconds at 30 second intervals for 5 min and centrifuged at 13.000 rpm for 15 min at 4 °C to pellet nuclei and cell debris. Protein lysates were boiled for 10 min and BCA assay was performed to measure protein concentration. Samples containing 12 - 30 µg of protein were heated at 95 °C for 5 min with 4x Bolt LDS sample buffer (Thermofisher, #B0007), supplemented with 5 % beta-mercaptoethanol, and loaded onto a 12% Bis-Tris plus gel (Thermofisher, #NW00122). The protein marker used was Precision Plus Protein™ Dual Color Standards, #1610374 (BioRad). Proteins were transferred onto a nitrocellulose membrane (Thermofisher, #88018) using a wet transfer system (Bio-Rad) according to manufacturer's instructions. Subsequent blocking and antibody incubation were performed in 5 % skimmed milk powder (#115363, Merck Millipore) in PBS containing 0.1% Tween-20. For the anti-p62 antibody, blocking was performed in 10% milk powder and antibody incubation in 1% milk powder in PBS containing 0.1% Tween-20. Antibodies used were: rabbit anti-LC3B (1:1000, Abcam, #ab51520), rabbit anti-p62 (1:1000, MBL, #PM045), rabbit anti-BECN1 (1:500, Santa Cruz, #sc-11427), rabbit anti-H3 (1:5000, Santa Cruz, #sc-10809), mouse anti-beta-actin (1:5000, Sigma, #A5441), mouse anti-Tubulin (1:500, Sigma, #T9026), rabbit anti-Atg5 (1:500, Novus, #NB110-53818). Secondary antibodies used were goat Anti-Mouse IgG (H+L)-HRP (1:10.000, BioRad, #1721011) and Goat Anti-Rabbit IgG (H+L)-HRP Conjugate (1:10.000, BioRad, #17210191). Membranes were developed using ECL (BioRad, #1705060), followed by chemiluminescence detection with a gel doc system (BioRad).

Immunohistochemistry and immunofluorescence

For transverse sections, larvae were fixed in 40 % ethanol, 5 % acetic acid and 10 % formalin for 3 h at room temperature followed by three washes in 70 % ethanol before being dehydrated following serial washes in Histoclear and reducing ethanol concentrations. Larvae were then sectioned at 5 µm intervals using a Reichert-Jung 2050 microtome (Leica). Sections were deparaffinized and hydrated following by 20 min of antigen retrieval in sodium citrate buffer pH 6.0 at 100 °C. Sections were blocked in 5% BSA in PBS- 0.1% Tween-20 for 1 h at room temperature and incubated overnight with sheep anti-p62 (1:200, Abcam, #ab31545) and rabbit anti-BECN1 (1:150, Santa Cruz, #sc-11427). Endogenous peroxidase activity was blocked in 0.3 % H_2O_2 for 20 min at room temperature followed by incubation with rabbit anti-sheep antibody (1:800, Abcam, #ab6747) for 1 h at room temperature. Sections were incubated with 0.1 M imidazole prior to detection with 3,3'-diaminobenzidine (DAB) substrate and counterstaining with hematoxylin.

For immunofluorescence, larvae were fixed in 4 % PFA overnight at 4°C, embedded vertically in a 0.5 % gelatin/30 % albumin mixture and sectioned at 120 µm intervals using a VT1000S vibratome (Leica). Sections were transferred to the wells of a 24-well plate containing PBD (PBS+0.1 % Tween-20 and 0.5 % Triton-X-100), which was then replaced with blocking solution (PBD + 1% BSA) for 1 h at RT. Sections were incubated with rabbit anti-LC3B (1:1000, abcam, #ab51520) in blocking solution overnight at 4 °C. Sections were washed three times for 15 min in PBS-0.1 % Tween-20 and incubated with secondary anti-rabbit 488 green fluorescent antibody (1:100, Thermofisher, #A11008) for 2 h at room temperature. Sections were then washed three times for 15 min in PBS-0.1 % Tween-20 prior to be incubated

with phalloidin-Alexa 588 (1:25, Thermofisher, #A12380) and DAPI (1:200, Thermofisher, #62248) for 30 min at room temperature in the dark and rinsed three times for 5 min with dH_2O. Sections were then imaged using the Zeiss LSM5 Exciter confocal laser-scanning microscope.

Equipment and settings

For immunohistochemistry, the sections were imaged on an upright compound Nikon Eclipse E800 microscope. The images were captured using a Nikon Digital Sight camera unit, equipped with a DS-Fi1 digital camera head and a DS-L2 camera controller. Pixel dimensions of the acquired images were W2584 X H1936 pixels, at 150 pixels/inch.

The magnification used was either 40X/0,75 magnification for anti-p62 staining (Figure 1) or 100X/1,4 magnification for anti-Becn1 staining (Supplementary Fig. S2).

The images were processed using Photoshop CS6 software. The original images were scaled-down constraining proportions, and cropped to the area of interest. Adjustment of Image Levels was applied on whole images. Assembly of the composite figures and labeling was done on Illustrator CC2015.

Confocal images were obtained in a sequential manner using a Zeiss LSM5 Exciter Confocal Laser Scanning Microscope equipped with Argon (458, 488, 514 nm), and 405, 450 and 635 diode excitation lasers and a 40× water immersion objective (C-APOCHROMAT 40×/1.2 Water). Emission ranges were set at 420-480, 505-550 and 560-615 nm in separate channels to prevent bleeding. Images were obtained using the Leica application X software (Leica, Wetzlar, Germany) and post-acquisition data analysis was performed using ImageJ software.

Morpholino injections

Translation-blocking morpholino (MO) directed against *atg5* (CATCCTTGTCATCTGCCATTATCAT) was obtained from Gene-Tools. The splice-blocking MO against *Sqstm1/p62* (CTTCATCTAGAGACAAAGTTCAGGA) was a kind gift from Prof. AM Meijer. Splice efficiency of *sqstm1* mRNA was tested in RT-PCR using a specific primer-set (Forward primer: 5' ATTTGCAGCGAAAAGTGCTC 3'; Reverse primer: 5' AGTGAACGGAAACCCAGGAA 3'). Embryos were injected at the 1-2-cell stage with either 2 ng (*atg5*) or 4 ng (*Sqstm1/p62*) of MO.

Drug treatments

Wild type or *lkb1*-mutant zebrafish embryos were treated from 1 dpf in embryo-medium at 28 °C with either of the following treatments: 50 µM calpeptin (Abcam, #4ab120804), 1 µM AR-12 (Medkoo Biosciences, #200272), or 10 µM rapamycin (Sigma, #R0395). Stock solutions of AR-12, rapamycin and calpeptin were prepared in DMSO and diluted in embryo medium for treatment (final concentration of DMSO, 0.2%). Other treatments were prepared in embryo medium. All treatments were refreshed every 2-3 days, larvae collected at the specified time points and genotyped for the *lkb1* gene. For Western Blotting, embryos were exposed to 2,5 µM chloroquine (Sigma, #C6628) for 14 h prior to lysing.

Statistics and quantification

Statistical significance was determined using Fisher's exact test in GraphPad software. Error bars represent the means ± standard errors of the means (SEM) and are pooled from a minimum of two independent experiments. A p-value of <0.05 was used to define statistical significance.

References

Boglev, Y., Badrock, A.P., Trotter, A.J., Du, Q., Richardson, E.J., Parslow, A.C., Markmiller, S.J., Hall, N.E., de Jong-Curtain, T.A., Ng, A.Y., et al. (2013). Autophagy induction is a Tor- and Tp53-independent cell survival response in a zebrafish model of disrupted ribosome biogenesis. PLoS Genet 9, e1003279.

Boya, P., Reggiori, F., and Codogno, P. (2013). Emerging regulation and functions of autophagy. Nature cell biology *15*, 713-720.

Chittaranjan, S., Bortnik, S., and Gorski, S.M. (2015). Monitoring Autophagic Flux by Using Lysosomal Inhibitors and Western Blotting of Endogenous MAP1LC3B. Cold Spring Harb Protoc 2015, 743-750.

Chiu, H.C., Soni, S., Kulp, S.K., Curry, H., Wang, D., Gunn, J.S., Schlesinger, L.S., and Chen, C.S. (2009). Eradication of intracellular Francisella tularensis in THP-1 human macrophages with a novel autophagy inducing agent. Journal of biomedical science *16*, 110.

Daouk, T., Larcher, T., Roupsard, F., Lyphout, L., Rigaud, C., Ledevin, M., Loizeau, V., and Cousin, X. (2011). Long-term food-exposure of zebrafish to PCB mixtures mimicking some environmental situations induces ovary pathology and impairs reproduction ability. Aquatic toxicology *105*, 270-278.

Dibble, C.C., and Cantley, L.C. (2015). Regulation of mTORC1 by PI3K signalling. Trends in cell biology *25*, 545-555.

Duran, A., Amanchy, R., Linares, J.F., Joshi, J., Abu-Baker, S., Porollo, A., Hansen, M., Moscat, J., and Diaz-Meco, M.T. (2011). p62 is a key regulator of nutrient sensing in the mTORC1 pathway. Molecular cell *44*, 134-146.

Efeyan, A., Zoncu, R., Chang, S., Gumper, I., Snitkin, H., Wolfson, R.L., Kirak, O., Sabatini, D.D., and Sabatini, D.M. (2013). Regulation of mTORC1 by the Rag GTPases is necessary for neonatal autophagy and survival. Nature *493*, 679-683.

Egan, D., Kim, J., Shaw, R.J., and Guan, K.L. (2011a). The autophagy initiating kinase ULK1 is regulated via opposing phosphorylation by AMPK and mTOR. Autophagy *7*, 643-644.

Egan, D.F., Shackelford, D.B., Mihaylova, M.M., Gelino, S., Kohnz, R.A., Mair, W., Vasquez, D.S., Joshi, A., Gwinn, D.M., Taylor, R., et al. (2011b). Phosphorylation of ULK1 (hATG1) by AMP-activated protein kinase connects energy sensing to mitophagy. Science *331*, 456-461.

Fleming, A., Noda, T., Yoshimori, T., and Rubinsztein, D.C. (2011). Chemical modulators of autophagy as biological probes and potential therapeutics. Nature chemical biology *7*, 9-17.

Galluzzi, L., Pietrocola, F., Levine, B., and Kroemer, G. (2014). Metabolic control of autophagy. Cell *159*, 1263-1276.

Gonzalez, A.A., Kumar, R., Mulligan, J.D., Davis, A.J., Weindruch, R., and Saupe, K.W. (2004). Metabolic adaptations to fasting and chronic caloric restriction in heart, muscle, and liver do not include changes in AMPK activity. American journal of physiology. Endocrinology and metabolism *287*, E1032-1037.

Gustafsson, J. (2009). Neonatal energy substrate production. The Indian journal of medical research *130*, 618-623.

Gut, P., Baeza-Raja, B., Andersson, O., Hasenkamp, L., Hsiao, J., Hesselson, D., Akassoglou, K., Verdin, E., Hirschey, M.D., and Stainier, D.Y. (2013). Whole-organism screening for gluconeogenesis identifies activators of fasting metabolism. Nature chemical biology *9*, 97-104.

Hardie, D.G., Ross, F.A., and Hawley, S.A. (2012). AMPK: a nutrient and energy sensor that maintains energy homeostasis. Nat Rev Mol Cell Biol *13*, 251-262.

Hawley, S.A., Boudeau, J., Reid, J.L., Mustard, K.J., Udd, L., Makela, T.P., Alessi, D.R., and Hardie, D.G. (2003). Complexes between the LKB1 tumor suppressor, STRAD alpha/beta and MO25 alpha/beta are upstream kinases in the AMP-activated protein kinase cascade. Journal of biology *2*, 28.

Heintz, N. (2004). Developmental biology: survival by self-digestion. Nature *432*, 963.

Hu, Z., Zhang, J., and Zhang, Q. (2011). Expression pattern and functions of autophagy-related gene atg5 in zebrafish organogenesis. Autophagy *7*, 1514-1527.

Kang, C., You, Y.J., and Avery, L. (2007). Dual roles of autophagy in the survival of Caenorhabditis elegans during starvation. Genes Dev *21*, 2161-2171.

Kim, J., Kundu, M., Viollet, B., and Guan, K.L. (2011). AMPK and mTOR regulate autophagy through direct phosphorylation of Ulk1. Nature cell biology *13*, 132-141.

Komatsu, M., Kurokawa, H., Waguri, S., Taguchi, K., Kobayashi, A., Ichimura, Y., Sou, Y.S., Ueno, I., Sakamoto, A., Tong, K.I., et al. (2010). The selective autophagy substrate p62 activates the stress responsive transcription factor Nrf2 through inactivation of Keap1. Nature cell biology *12*, 213-223.

Kroemer, G., Marino, G., and Levine, B. (2010). Autophagy and the integrated stress response. Molecular cell *40*, 280-293.

Kuma, A., Hatano, M., Matsui, M., Yamamoto, A., Nakaya, H., Yoshimori, T., Ohsumi, Y., Tokuhisa, T., and Mizushima, N. (2004). The role of autophagy during the early neonatal starvation period. Nature *432*, 1032-1036.

Laderoute, K.R., Amin, K., Calaoagan, J.M., Knapp, M., Le, T., Orduna, J., Foretz, M., and Viollet, B. (2006). 5'-AMP-activated protein kinase (AMPK) is induced by low-oxygen and glucose deprivation conditions found in solid-tumor microenvironments. Mol Cell Biol *26*, 5336-5347.

Lamark, T., Kirkin, V., Dikic, I., and Johansen, T. (2009). NBR1 and p62 as cargo receptors for selective autophagy of ubiquitinated targets. Cell Cycle *8*, 1986-1990.

Laplante, M., and Sabatini, D.M. (2012). mTOR signalling in growth control and disease. Cell *149*, 274-293.

Lee, E., Koo, Y., Ng, A., Wei, Y., Luby-Phelps, K., Juraszek, A., Xavier, R.J., Cleaver, O., Levine, B., and Amatruda, J.F. (2014). Autophagy is essential for cardiac morphogenesis during vertebrate development. Autophagy *10*, 572-587.

Liang, J., Shao, S.H., Xu, Z.X., Hennessy, B., Ding, Z., Larrea, M., Kondo, S., Dumont, D.J., Gutterman, J.U., Walker, C.L., et al. (2007). The energy sensing LKB1-AMPK pathway regulates p27(kip1) phosphorylation mediating the decision to enter autophagy or apoptosis. Nat Cell Biol *9*, 218-224.

Lizcano, J.M., Goransson, O., Toth, R., Deak, M., Morrice, N.A., Boudeau, J., Hawley, S.A., Udd, L., Makela, T.P., Hardie, D.G., et al. (2004). LKB1 is a master kinase that activates 13 kinases of the AMPK subfamily, including MARK/PAR-1. The EMBO journal *23*, 833-843.

Maiuri, M.C., Tasdemir, E., Criollo, A., Morselli, E., Vicencio, J.M., Carnuccio, R., and Kroemer, G. (2009). Control of autophagy by oncogenes and tumor suppressor genes. Cell Death Differ *16*, 87-93.

Makky, K., Tekiela, J., and Mayer, A.N. (2007). Target of rapamycin (TOR) signalling controls epithelial morphogenesis in the vertebrate intestine. Dev Biol *303*, 501-513.

Marshall, K.E., Tomasini, A.J., Makky, K., S, N.K., and Mayer, A.N. (2010). Dynamic Lkb1-TORC1 signalling as a possible mechanism for regulating the endoderm-intestine transition. Dev Dyn *239*, 3000-3012.

Meyer, G., Czompa, A., Reboul, C., Csepanyi, E., Czegledi, A., Bak, I., Balla, G., Balla, J., Tosaki, A., and Lekli, I. (2013). The cellular autophagy markers Beclin-1 and LC3B-II are increased during reperfusion in fibrillated mouse hearts. Current pharmaceutical design *19*, 6912-6918.

Mizushima, N., and Klionsky, D.J. (2007). Protein turnover via autophagy: implications for metabolism. Annual review of nutrition *27*, 19-40.

Mizushima, N., Levine, B., Cuervo, A.M., and Klionsky, D.J. (2008). Autophagy fights disease through cellular self-digestion. Nature *451*, 1069-1075.

Mizushima, N., and Yoshimori, T. (2007). How to interpret LC3 immunoblotting. Autophagy *3*, 542-545.

Moscat, J., and Diaz-Meco, M.T. (2009). p62 at the crossroads of autophagy, apoptosis, and cancer. Cell *137*, 1001-1004.

Moscat, J., and Diaz-Meco, M.T. (2011). Feedback on fat: p62-mTORC1-autophagy connections. Cell *147*, 724-727.

Narbonne, P., and Roy, R. (2009). Caenorhabditis elegans dauers need LKB1/AMPK to ration lipid reserves and ensure long-term survival. Nature *457*, 210-214.

Orhon, I., Dupont, N., Zaidan, M., Boitez, V., Burtin, M., Schmitt, A., Capiod, T., Viau, A., Beau, I.,

Kuehn, E.W., et al. (2016). Primary-cilium-dependent autophagy controls epithelial cell volume in response to fluid flow. Nature cell biology *18*, 657-667.

Pilkis, S.J., and Granner, D.K. (1992). Molecular physiology of the regulation of hepatic gluconeogenesis and glycolysis. Annual review of physiology *54*, 885-909.

Polak, P., and Hall, M.N. (2009). mTOR and the control of whole body metabolism. Current opinion in cell biology *21*, 209-218.

Rabinowitz, J.D., and White, E. (2010). Autophagy and metabolism. Science *330*, 1344-1348.

Rusten, T.E., and Stenmark, H. (2010). p62, an autophagy hero or culprit? Nature cell biology *12*, 207-209.

Schlegel, A., and Gut, P. (2015). Metabolic insights from zebrafish genetics, physiology, and chemical biology. Cellular and molecular life sciences : CMLS.

Schlegel, A., and Stainier, D.Y. (2007). Lessons from "lower" organisms: what worms, flies, and zebrafish can teach us about human energy metabolism. PLoS Genet *3*, e199.

Scott, R.C., Schuldiner, O., and Neufeld, T.P. (2004). Role and regulation of starvation-induced autophagy in the Drosophila fat body. Developmental cell *7*, 167-178.

Seth, A., Stemple, D.L., and Barroso, I. (2013). The emerging use of zebrafish to model metabolic disease. Dis Model Mech *6*, 1080-1088.

Shaw, R.J., Bardeesy, N., Manning, B.D., Lopez, L., Kosmatka, M., DePinho, R.A., and Cantley, L.C. (2004a). The LKB1 tumor suppressor negatively regulates mTOR signalling. Cancer Cell *6*, 91-99.

Shaw, R.J., Kosmatka, M., Bardeesy, N., Hurley, R.L., Witters, L.A., DePinho, R.A., and Cantley, L.C. (2004b). The tumor suppressor LKB1 kinase directly activates AMP-activated kinase and regulates apoptosis in response to energy stress. Proc Natl Acad Sci U S A *101*, 3329-3335.

Shintani, T., and Klionsky, D.J. (2004). Autophagy in health and disease: a double-edged sword. Science *306*, 990-995.

Subramani, S., and Malhotra, V. (2013). Non-autophagic roles of autophagy-related proteins. EMBO Rep *14*, 143-151.

Sugawara, K., Suzuki, N.N., Fujioka, Y., Mizushima, N., Ohsumi, Y., and Inagaki, F. (2004). The crystal structure of microtubule-associated protein light chain 3, a mammalian homologue of Saccharomyces cerevisiae Atg8. Genes Cells *9*, 611-618.

van der Vaart, M., Korbee, C.J., Lamers, G.E., Tengeler, A.C., Hosseini, R., Haks, M.C., Ottenhoff, T.H., Spaink, H.P., and Meijer, A.H. (2014). The DNA damage-regulated autophagy modulator DRAM1 links mycobacterial recognition via TLP-MYD88 to authophagic defense. Cell host & microbe *15*, 753-767.

van der Velden, Y.U., Wang, L., Zevenhoven, J., van Rooijen, E., van Lohuizen, M., Giles, R.H., Clevers, H., and Haramis, A.P. (2011). The serine-threonine kinase LKB1 is essential for survival under energetic stress in zebrafish. Proc Natl Acad Sci U S A *108*, 4358-4363.

Varga, M., Fodor, E., and Vellai, T. (2015). Autophagy in zebrafish. Methods *75*, 172-180.

Varga, M., Sass, M., Papp, D., Takacs-Vellai, K., Kobolak, J., Dinnyes, A., Klionsky, D.J., and Vellai, T. (2014). Autophagy is required for zebrafish caudal fin regeneration. Cell Death Differ *21*, 547-556.

Viollet, B., Guigas, B., Leclerc, J., Hebrard, S., Lantier, L., Mounier, R., Andreelli, F., and Foretz, M. (2009). AMP-activated protein kinase in the regulation of hepatic energy metabolism: from physiology to therapeutic perspectives. Acta physiologica *196*, 81-98.

Wienholds, E., van Eeden, F., Kosters, M., Mudde, J., Plasterk, R.H., and Cuppen, E. (2003). Efficient target-selected mutagenesis in zebrafish. Genome Res *13*, 2700-2707.

Williams, A., Sarkar, S., Cuddon, P., Ttofi, E.K., Saiki, S., Siddiqi, F.H., Jahreiss, L., Fleming, A., Pask, D., Goldsmith, P., et al. (2008). Novel targets for Huntington's disease in an mTOR-independent autophagy pathway. Nat Chem Biol *4*, 295-305.

Ylikorkala, A., Rossi, D.J., Korsisaari, N., Luukko, K., Alitalo, K., Henkemeyer, M., and Makela, T.P. (2001). Vascular abnormalities and deregulation of VEGF in Lkb1-deficient mice. Science *293*, 1323-1326.

Yousefi, S., Perozzo, R., Schmid, I., Ziemiecki, A., Schaffner, T., Scapozza, L., Brunner, T., and Simon, H.U. (2006). Calpain-mediated cleavage of Atg5 switches autophagy to apoptosis. Nature cell biology *8*, 1124-1132.

Acknowledgments

We thank Prof. Annemarie Meijer for the *sqstm1/p62* morpholino and critical advice on the manuscript, Gerda Lamers (IBL) for advice with confocal microscopy, the DNA-Markerpoint facility (IBL) for genotyping, and the animal caretakers for excellent care of the fish. We also thank Dr. Anastassis Perrakis (NKI) for critical reading of the manuscript and the Life Science Editors for editorial assistance. The work was supported by a grant from the Dutch Cancer Society (KWF UL 2012-5395) to A-P.G.H.

Supplementary Figures

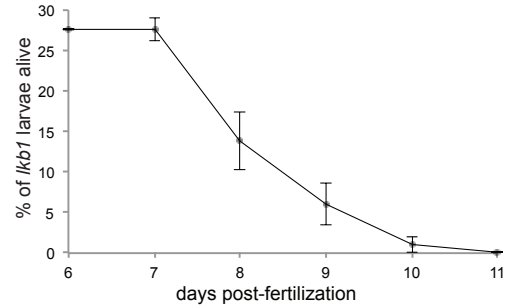

Figure S1. The majority of *lkb1* larvae die from premature starvation at 7-8 dpf. Larvae were collected from pairings of *lkb1* heterozygotes. 100 alive larvae/time-point were collected and genotyped for the *lkb1* mutation at 6, 7, 8, 9 and 10 dpf. The percentage of *lkb1* larvae alive in the total population is plotted on each time-point. Error bars represent the means ± standard errors of the means (SEM) and are pooled from three independent experiments. The graph depicts that *lkb1* larvae start dying at 7 dpf, the majority of *lkb1* larvae die at 8 dpf and very few "escapers" are alive at 9 dpf.

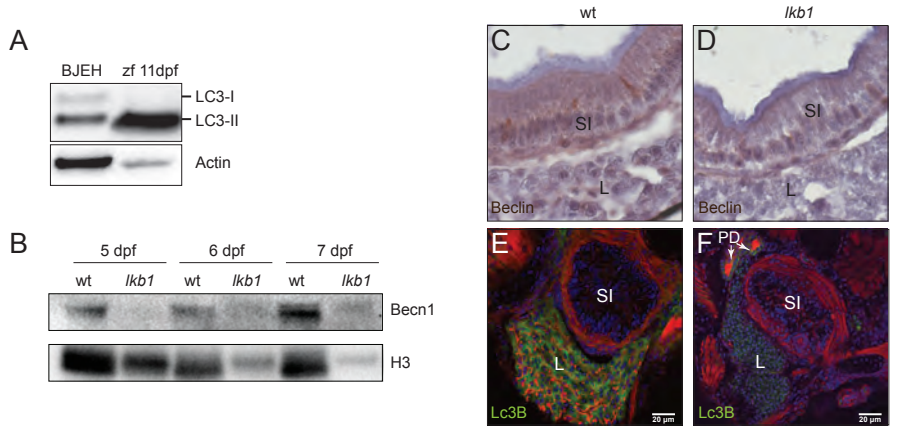

Figure S2. Autophagy markers Lc3B and Beclin are lower in *lkb1* larvae. (A) The LC3B antibody recognizes the cleaved Lc3-II in zebrafish. Western blot analysis using antibodies against LC3B and beta-actin (loading control) on total protein lysates from human BJEH cells that were serum-starved overnight and wt zebrafish larvae at 11 dpf. The LC3B antibody recognizes the uncleaved and cleaved forms of LC3B in the human sample but predominantly the cleaved Lc3-II in the zebrafish sample. **(B)** Western blot analysis of Beclin (Becn1) and Histone H3 (loading control) in total protein lysates of wt and *lkb1* trunks between 5-7 dpf. Larvae were treated with chloroquine (2.5 µM) for 14 h prior to processing. Becn1 levels are lower in the *lkb1* larvae at all time-points. **(C-D)** Immunohistochemical analysis of transverse paraffin sections (5µm) of intestine of 7 dpf wt and *lkb1* larvae shows very low levels of Becn1 expression in the *lkb1* intestine. Magnification: 100X. (E-F) Transverse vibratome sections (150 µm) of liver of 7 dpf wt and *lkb1* larvae stained with anti-LC3B antibody (green), rhodamine-phalloidin to detect F-actin (red) and DAPI to detect nuclei (blue). Lc3B staining in the lkb1 liver is greatly reduced. PD: pronephric ducts; L: liver; SI: intestine.

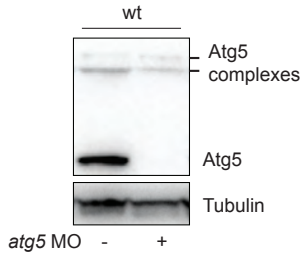

Figure S3. The atg5MO efficiently inhibits Atg5 translation. Western blot analysis of wt larvae at 4 dpf, with an antibody against Atg5. Tubulin is used as a loading control. Atg5 expression is almost undetectable in larvae injected with 0,5 µM atg5MO at the one-cell stage, showing efficient inhibition of Atg5 translation.

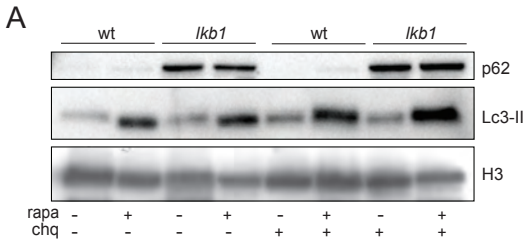

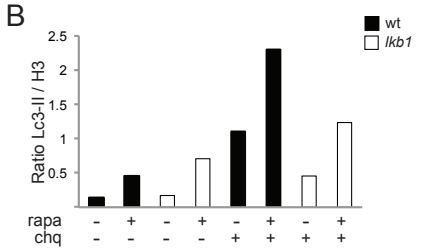

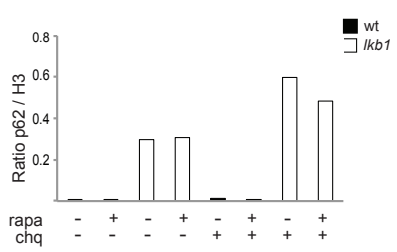

Figure S4. Rapamycin treatment leads to increased Lc3-II accumulation but does not restore p62 degradation in *lkb1* larvae. (A) Western Blot analysis of p62, Lc3-II, and histone H3 (loading control) in total protein lysates of wt and lkb1 trunks at 6 dpf that were treated with either 10µM rapamycin from 24 hpf or DMSO (negative control). To detect the autophagic flux the larvae were treated or not with 2.5 µM chloroquine for 14 h prior to processing. Rapamycin treatment leads to increased Lc3-II levels in both wt and *lkb1* larvae, but p62 levels remained high in *lkb1* larvae. **(B)** Graphical representation of the data shown in **(A)**, depicting the densitometric p62/H3 and Lc3-II/H3 ratios. **(C)** Representative image of a wt larva at 6 dpf that has been treated with 10µM rapamycin from 24 hpf onwards. Note the high amount of yolk still present indicating developmental delay.

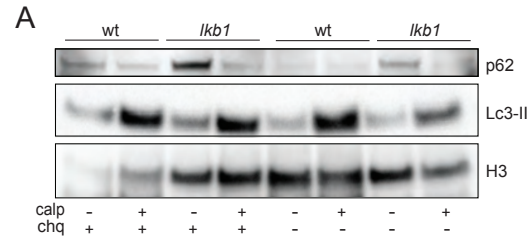

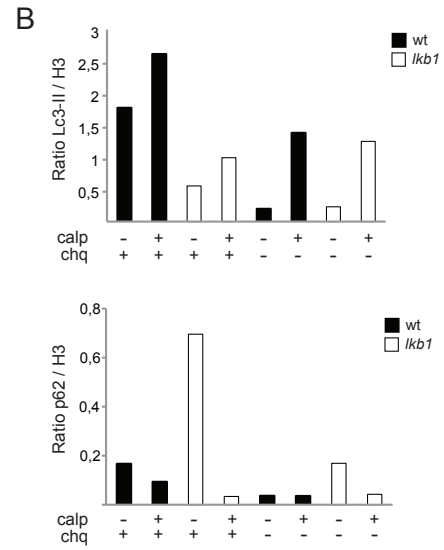

Figure S5. Calpeptin-mediated activation of autophagy restores p62 degradation in *lkb1* larvae. (A) Western blot analysis of Lc3-II, p62 and Histone H3 (loading control) in total protein lysates of wt and *lkb1* trunks at 6 dpf. The embryos were treated with 50 µM calpeptin or DMSO (negative control) from 1 dpf onwards. To detect the autophagic flux, larvae were treated or not with 2.5 µM chloroquine for 14 h prior to lysing. Calpeptin treatment leads to upregulation of Lc3-II levels in both wt and *lkb1* larvae. Induction of autophagy by calpeptin also leads to robust downregulation of p62 accumulation in *lkb1* larvae. **(B)** Graphical representation of the data shown in **(A)**, depicting the densitometric p62/H3 and Lc3-II/H3 ratios.

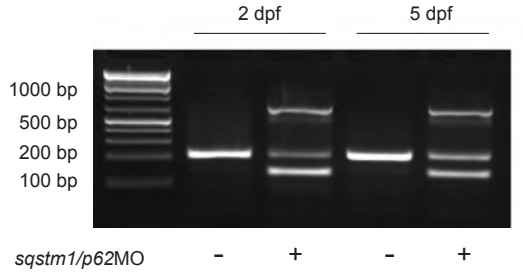

Figure S6. The sqstm1/p62MO efficiently blocks splicing of sqstm1/p62 mRNA. Reverse transcription polymerase chain reaction (RT-PCR) was used to confirm antisense morpholino blocking of intron-exon splicing events in zebrafish *sqstm1/p62* mRNA at 2 and 5 dpf. Upon injection of 0,5 mM *sqstm1/p62* MO (i1e2, targeting splicing between the first intron and the second exon), the 200 bp RT-PCR product is disrupted.